

# Origin of the $p$ -process radionuclides $^{92}\text{Nb}$ and $^{146}\text{Sm}$ in the early Solar System and inferences on the birth of the Sun

Maria Lugaro <sup>\*</sup> †, Marco Pignatari <sup>\*</sup> ‡, Ulrich Ott <sup>§</sup> ¶, Kai Zuber <sup>||</sup>, Claudia Travaglio <sup>\*\*</sup> ‡, György Gyürky <sup>††</sup>, and Zsolt Fülöp <sup>††</sup>

<sup>\*</sup>Konkoly Observatory, Research Centre for Astronomy and Earth Sciences, Hungarian Academy of Sciences, H-1121 Budapest, Hungary, <sup>†</sup>Monash Centre for Astrophysics, Monash University, VIC3800, Australia, <sup>‡</sup>Nugrid collaboration, <sup>§</sup>Faculty of Natural Science, University of West Hungary, H-9700 Szombathely, Hungary, <sup>¶</sup>Max-Planck Institute for Chemistry, D-55128 Mainz, Germany, <sup>||</sup>Institut für Kern- und Teilchenphysik, Technische Universität Dresden, D-01069 Dresden, Germany, <sup>\*\*</sup>Osservatorio di Torino, I-10025, Pino Torinese, Italy, and <sup>††</sup>Atomki Institute for Nuclear Research, Hungarian Academy of Sciences, H-4001, Debrecen, Hungary

Submitted to Proceedings of the National Academy of Sciences of the United States of America

**The abundances of  $^{92}\text{Nb}$  and  $^{146}\text{Sm}$  in the early Solar System are determined from meteoritic analysis and their stellar production is attributed to the  $p$  process. We investigate if their origin from thermonuclear supernovae deriving from the explosion of white dwarfs with mass above the Chandrasekhar limit is in agreement with the abundance of  $^{53}\text{Mn}$ , another radionuclide present in the early Solar System and produced in the same events. A consistent solution for  $^{92}\text{Nb}$  and  $^{53}\text{Mn}$  cannot be found within the current uncertainties and requires that the  $^{92}\text{Nb}/^{92}\text{Mo}$  ratio in the early Solar System is at least 50% lower than the current nominal value, which is outside its present error bars. A different solution is to invoke another production site for  $^{92}\text{Nb}$ , which we find in the  $\alpha$ -rich freezeout during core-collapse supernovae from massive stars. Whichever scenario we consider, we find that a relatively long time interval of at least  $\sim 10$  Myr must have elapsed from when the star-forming region where the Sun was born was isolated from the interstellar medium and the birth of the Sun. This is in agreement with results obtained from radionuclides heavier than iron produced by neutron captures and lends further support to the idea that the Sun was born in a massive star-forming region together with many thousands of stellar siblings.**

short-lived radionuclides | Solar System formation | supernovae

**R**adionuclides with half lives of the order of 1 to 100 million years (Myr) were present in the early Solar System (ESS) and represent a clue to investigate the circumstances of the birth of the Sun [1]. The abundances of some of these nuclei in the ESS, as inferred from analysis of meteorites and reported relative to the abundance of a stable nucleus, are given with error bars as low as a few percent. However, our ability to exploit radionuclides as chronometer for the events that led to the birth of the Sun is undermined by the fact that our understanding of their production by nuclear reactions in stars is still relatively poor. This is because it relies on stellar models that include highly uncertain physics related to, e.g., mixing, the mechanisms of supernova explosions, and nuclear reaction rates. Here we focus on the origin of radionuclides heavier than Fe. Among them,  $^{92}\text{Nb}$ ,  $^{129}\text{I}$ ,  $^{146}\text{Sm}$ , and  $^{182}\text{Hf}$  have abundances in the ESS known with error bars lower than 20%. Lugaro *et al.* [2] recently proposed a decoupled origin for  $^{129}\text{I}$  and  $^{182}\text{Hf}$ : The former was produced by *rapid* neutron captures ( $r$  process) in a supernova or neutron star merger roughly 100 Myr before the formation of the Sun, and the latter by *slow* neutron captures ( $s$  process) in an asymptotic giant branch star roughly 10–30 Myr before the formation of the Sun. From these timescales it was concluded that the star forming region where the Sun was born may have lived for a few tens of million years, which is possible only if such a region was very massive and gave birth to many hundreds of stellar siblings [3].

Here, we turn to the investigation of the origin of the other two radionuclides heavier than Fe whose abundances are well

known in the ESS:  $^{92}\text{Nb}$  and  $^{146}\text{Sm}$ . These nuclei are proton rich, relative to the stable nuclei of Nb and Sm, which means that they cannot be produced by neutron captures like the vast majority of the nuclei heavier than Fe. Instead, their nucleosynthetic origin has been traditionally ascribed to some flavor of the so-called  $p$  process [4, 5], for example, the disintegration of heavier nuclei ( $\gamma$  process). Unfortunately, the possible astrophysical sites of origin of  $p$ -process nuclei in the Universe are not well constrained.

Core-collapse supernova explosions (CCSNe [6]) deriving from the final collapse of massive stars have been considered as a possible site for the  $\gamma$  process, specifically, occurring in the O-Ne-rich zones of the CCSN ejecta [7]. However, models never managed to reproduce the complete  $p$ -process pattern observed in the bulk of the Solar System material [8, 9, 10]. For instance, CCSN models cannot reproduce the relatively large abundances of  $^{92,94}\text{Mo}$  and  $^{96,98}\text{Ru}$ . Taking into account nuclear uncertainties has not solved the problem [11, 12], except for a possible increase of the  $^{12}\text{C}+^{12}\text{C}$  fusion reaction rate [13, 14]. Another process in CCSNe that can produce the light  $p$ -process nuclei up to Pd-Ag, including  $^{92}\text{Nb}$ , is the combination of  $\alpha$ , proton, neutron captures, and their reverse reactions in  $\alpha$ -rich freezeout conditions [15]. Neutrino winds from the forming neutron star are also a possible site for the production of the light  $p$ -process nuclei [16, 17, 18], although,

## Significance

Radioactive nuclei with half lives of the order of million of years were present in the Solar System at its birth and can be used as clocks to measure the events that predated the birth of the Sun. Two of these nuclei are heavy and rich in protons and can be produced only by particular chains of nuclear reactions during some supernova explosions. We have used their abundances to derive that at least 10 million years passed between the last of these explosions and the birth of the Sun. This means that the region where the Sun was born must have lived at least as long, which is possible only if it was very massive.

Reserved for Publication Footnotes

one of its possible components (the so-called  $\nu p$ -process [19]) cannot produce  $^{92}\text{Nb}$  because it is shielded by  $^{92}\text{Mo}$  [5, 20]. The same occurs in the case of the  $r p$ -process in X-ray bursts [21]. Neutrino-induced reactions in CCSNe (the  $\nu$ -process) can also produce some  $^{92}\text{Nb}$  [22], but no other  $p$ -process nuclei.

Thermonuclear supernovae (SNeIa) deriving from the explosion of a white dwarf that accreted material from a main sequence companion to above the Chandrasekhar limit have been proposed as a site of the  $\gamma$  process [23, 24, 25]. In these models, heavy seed nuclei are assumed to be produced by the  $s$  process during the accretion phase and, given a certain initial  $s$ -process distribution, it is possible to reproduce the high abundances of  $^{92,94}\text{Mo}$  and  $^{96,98}\text{Ru}$  in the Solar System. However, there are still many uncertainties related to the origin and the features of the neutron-capture processes activated during the white dwarf accretion leading to SNIa. Recently, Travaglio *et al.* [26] (hereafter TR14) analyzed in detail the production of  $^{92}\text{Nb}$  and  $^{146}\text{Sm}$  in SNeIa using multidimensional models and concluded that such an origin is plausible for both radionuclides in the ESS. Here, we consider these results and combine them with new predictions of the production of  $p$ -process nuclei in  $\alpha$ -rich freezeout conditions in CCSNe to investigate the origin of  $^{92}\text{Nb}$  and  $^{146}\text{Sm}$  and to use it to further constrain the circumstances of the birth of the Sun.

### Abundance ratios and related timescales

In simple analytic terms the abundance ratio of a short-lived ( $T_{1/2} < 100$  Myr) radioactive to a stable isotope in the material that ended up in the Solar System, just after a given nucleosynthetic event and assuming that both nuclides are only produced by this type of event, can be derived using the formula [2, 27]:

$$\frac{N_{radio}}{N_{stable}} = K \times \frac{p_{radio}}{p_{stable}} \times \frac{\delta}{T} \times \left( 1 + \frac{e^{-\delta/\tau}}{1 - e^{-\delta/\tau}} \right), \quad [1]$$

where  $p_{radio}/p_{stable}$  is the production ratio of each single event,  $\tau$  is the mean life ( $=T_{1/2}/\ln 2$ ) of the radionuclide,  $T$  the timescale of the evolution of the Galaxy up to the formation of the Sun ( $\sim 10^{10}$  yr), and  $\delta$  the recurrence time between each event. The value of  $\delta$  is essentially a free parameter that may vary between 10 and 100 Myr [28]. The number  $K$  is also a free parameter that accounts for the effect of infall of low-metallicity gas, which dilutes the abundances, and the fact that a fraction of the abundances produced, particularly for stable isotopes, is locked inside stars [29]. The value of  $K$  changes depending on whether the isotopes involved are of primary or secondary origin, i.e., whether they are produced from the H and He abundances in the star or depend on the initial presence of CNO elements, respectively. These effects are complex to evaluate analytically, but the general result is that  $K > 1$  [30]. Lugaro *et al.* [2] did not consider the number  $K$  in their evaluation of ratios from Eq. 1, which means that effectively they used  $K=1$  and their reported timescales represent conservative lower limits.

TR14 did not use Eq. 1, but included the yields of  $^{92}\text{Nb}$ ,  $^{97}\text{Tc}$ ,  $^{98}\text{Tc}$ , and  $^{146}\text{Sm}$  (and their reference isotopes  $^{92}\text{Mo}$ ,  $^{98}\text{Ru}$ , and  $^{144}\text{Sm}$ ) from their SNIa models into full, self-consistent Galactic chemical evolution (GCE) simulations to evaluate the abundance ratios  $^{92}\text{Nb}/^{92}\text{Mo}$ ,  $^{97}\text{Tc}/^{98}\text{Ru}$ ,  $^{98}\text{Tc}/^{98}\text{Ru}$ , and  $^{146}\text{Sm}/^{144}\text{Sm}$  in the interstellar medium (ISM) at the time of the birth of the Sun, assuming that the production of  $p$  nuclei only occurs in SNIa. These detailed models reproduce the abundances of the stable reference isotopes considered here [25]. With Eq. 1 we can recover re-

sults close to those of the detailed GCE models for the four ratios considered here using as  $p_{radio}/p_{stable}$  the average of the values given in Table 1 of TR14<sup>1</sup>,  $T = 9200$  Myr from TR14,  $\delta = 8$  Myr, and  $K = 2$  (Table 1). This means that roughly  $(1/K)(T/\delta) \simeq 600$  SNIa  $p$ -process events contributed to the Solar System abundances of the stable isotopes considered here. For the unstable isotopes, it depends on their mean life: because  $^{97}\text{Tc}$  and  $^{98}\text{Tc}$  have relatively short mean lives, the second term of the sum in Eq. 1 representing the memory of all the events prior the last event counts for 26% of the total, hence, most of their ESS abundances come from the last event. On the other hand, for  $^{92}\text{Nb}$  and  $^{146}\text{Sm}$ , due to their long half lives, the second term of the sum is the most important. For example, in the case of  $^{92}\text{Nb}$  it accounts for 85% of the total amount of  $^{92}\text{Nb}$ . In these cases the ratios from Eq. 1 are very close to the corresponding ISM steady-state ratio, i.e., the production ratio multiplied by  $K\tau/T$ .

Although we can recover the values of the ratios produced by the full GCE models using Eq. 1, we need to keep in mind some distinctions. The ratios derived by TR14 using the full GCE model represent values at an absolute time 9200 Myr from the birth of the Galaxy, when the ISM reaches solar metallicity. From these values, we can evaluate an isolation timescale ( $T_{\text{isolation}}$ ): the interval between the time when the material that ended up in the Solar System became isolated from the ISM and the time of the formation of the Solar System.  $T_{\text{isolation}}$  is derived such that the ratio between the ESS ratio and the ISM ratio for a given radioactive and stable pair is simply given by  $e^{-T_{\text{isolation}}/\tau}$ . In reality, however, some mixing could have occurred. An ISM mixing timescale ( $T_{\text{mixing}}$ ) between different phases of the ISM should be of the order of 10 - 100 Myr. The effect of such process was analytically investigated by [31], from which [5] derived that the ratio between the ESS ratio and the ISM ratio for a given radioactive and stable pair is given by  $1 + 1.5x + 0.4x^2$ , where  $x = T_{\text{mixing}}/\tau$ . In this picture, the requirement is that the composition of the star-forming region where the Sun was born must have been affected by mixing with the ISM, hence,  $T_{\text{mixing}}$  represents a lower limit for  $T_{\text{isolation}}$ .

Values derived using Eq. 1, instead, represent ratios in the matter that built up the Solar System just after the last, final addition from a nucleosynthetic event. From them, we can evaluate a last-event timescale ( $T_{\text{last}}$ ): the interval between the time of the last event and the time of the formation of the Solar System.  $T_{\text{last}}$  represents an upper limit of  $T_{\text{isolation}}$  and is derived such that the ratio between the ESS ratio and the ISM ratio for a given radioactive and stable pair is simply given by  $e^{-T_{\text{last}}/\tau}$  (as for  $T_{\text{isolation}}$ ). The more  $\delta/\tau$  is lower than unity, the closer the ratio derived from Eq. 1 is to the ISM ratio, and the closer  $T_{\text{last}}$  to  $T_{\text{isolation}}$ . The main drawback of this approach is that the  $K$  and the  $\delta$  values in Eq. 1 are uncertain. The advantages are that there are not further complications with regards to mixing in the ISM and that this description is relatively free from uncertainties related to the setting of the time of the birth of the Sun. In the model of TR14, this is defined as the time when the Galactic metallicity reaches the solar value. However, stellar ages and metallicities in the Galaxy are not strictly correlated [32]. Chemodynamical GCE models also including the effect of stellar migration [33, 34] are required to obtain the observed spread, but have not been applied to the evolution of radioactive nuclei yet.

<sup>1</sup>We average only the values given for metallicities in the range  $Z = 0.01 - 0.02$ , since we are focusing on events that occurred close in time to the formation of the Sun. Variations in this range of  $Z$  are within 25%. When considering also  $Z$  down to 0.003 they are within a factor of 2. The only exception is  $^{98}\text{Tc}/^{98}\text{Ru}$ , which varies by 50% in the range  $Z = 0.01 - 0.02$  and by a factor of 6 when also considering  $Z = 0.003$ .

We expect these models to produce a range of abundances of the radioactive nuclei at any given metallicity, but we cannot predict based on first principles if these variations will be significant. Finally, it should be noted that, while  $T_{\text{isolation}}$  and  $T_{\text{mixing}}$  are required to be the same for all the different types of nucleosynthetic events that contributed to the Solar System matter,  $T_{\text{last}}$  is in principle different for each type of event.

### The SNIa source

We evaluate  $T_{\text{isolation}}$  and  $T_{\text{mixing}}$  assuming that the  $p$ -process radionuclides were produced by SNeIa and comparing the abundance ratios obtained by TR14 to those observed in the ESS (Table 1). TR14 carefully analysed the nuclear uncertainties that affect the production of  $^{92}\text{Nb}$  and  $^{146}\text{Sm}$  in SNeIa. In the production of  $^{92}\text{Nb}$ ,  $(\gamma, n)$  reactions play the dominant role with some contribution from proton induced reactions. The nuclear uncertainties are related to the choice of the  $\gamma$ -ray strength function and, to a lesser extent, the proton-nucleus optical potential. Since the rates of some of the most important reactions are constrained experimentally, the nuclear uncertainties on the  $^{92}\text{Nb}$  production are moderate, resulting in possible variations in the ISM ratio of less than a factor of two. The  $^{146}\text{Sm}/^{144}\text{Sm}$  ratio, on the other hand, is determined by  $(\gamma, n)/(\gamma, \alpha)$  branchings, mainly on  $^{148}\text{Gd}$ . The uncertainty range reported by TR14 is based on three choices of the  $^{148}\text{Gd}(\gamma, \alpha)^{144}\text{Sm}$  rate. With respect to two previous estimates [35, 36], the new rate of [37] results in a  $^{146}\text{Sm}/^{144}\text{Sm}$  ratio higher by a factor of two in SNIa, but lower by at least a factor of two in CCSNe [37]. Realistically, the  $^{146}\text{Sm}/^{144}\text{Sm}$  ratio may have an even higher nuclear uncertainty, possibly up to one order of magnitude, owing to the lack of experimental data at the relevant low energies for the  $^{148}\text{Gd}(\gamma, \alpha)^{144}\text{Sm}$  rate itself and for the low energy  $\alpha$ -nucleus optical potential required for the extrapolation [38]. For  $^{92}\text{Nb}/^{92}\text{Mo}$ , if we compare the maximum value allowed within nuclear uncertainties of  $3.12 \times 10^{-5}$  to the lower limit of the ESS value, we derive a maximum  $T_{\text{isolation}}$  of 5.4 Myr and a maximum  $T_{\text{mixing}}$  of 3.7 Myr. It is also possible to recover a solution for  $^{146}\text{Sm}/^{144}\text{Sm}$  consistent with these values, given the large uncertainties. Currently, the value of the half life of  $^{146}\text{Sm}$  is debated between the two values of 68 and 103 Myr [39, 40]. Here, we have used the lower value, if we used the higher value we would obtain longer timescales than those reported in Table 1.

We extend the study of TR14 to investigate if the origin of  $^{92}\text{Nb}$  and  $^{146}\text{Sm}$  is compatible with that of the radionuclide  $^{53}\text{Mn}$ . This nucleus provides us a strong constraint because near Chandrasekhar-mass SNeIa are also the major producers of Mn in the Solar System [41] and, together with the stable  $^{55}\text{Mn}$ , they produce  $^{53}\text{Mn}$ , whose solar abundance is well determined in the ESS (Table 1). We calculate the ISM  $^{53}\text{Mn}/^{55}\text{Mn}$  ratio from Eq. 1 using the same values for  $\delta$ ,  $K$ , and  $T$  derived above and the production ratio  $^{53}\text{Mn}/^{55}\text{Mn}=0.108$  predicted by the same SNIa model used to derive the  $p$ -process abundances. This is derived from the  $^{53}\text{Cr}$  abundance given by [24], but, we note that different models produce very similar  $^{53}\text{Mn}/^{55}\text{Mn}$  ratios [42]. We calculate an ISM  $^{53}\text{Mn}/^{55}\text{Mn}$  ratio of  $2.41 \times 10^{-4}$ , which, after an isolation time of 5.4 Myr, results in a ratio of  $5.82 \times 10^{-5}$ , one order of magnitude higher than the ESS value. An isolation time of at least 19 Myr is instead required to match the  $^{53}\text{Mn}/^{55}\text{Mn}$  constraint. If we make the conservative assumption that  $K=1$ , instead of 2, to calculate the ISM  $^{53}\text{Mn}/^{55}\text{Mn}$  ratio from Eq. 1 we obtain  $T_{\text{isolation}} \simeq 15$  Myr. This value is strongly incompatible with the upper limit of 5.4 Myr required to match the

$^{92}\text{Nb}/^{92}\text{Mo}$ , in other words, SNIa nucleosynthesis results in too high production of  $^{53}\text{Mn}$  relative to  $^{92}\text{Nb}$ , and to their ESS abundances.

A three times lower  $^{53}\text{Mn}/^{55}\text{Mn}$  ratio in SNIa would result from a tenfold increase of the  $^{32}\text{S}(\beta^+)^{32}\text{P}$  decay [43], in which case  $T_{\text{isolation}}$  would decrease to  $\simeq 9$  Myr. This possibility needs to be further investigated. On the other hand, a possibly longer half life for  $^{53}\text{Mn}$  (see discussion in [44]) would further increase the difference. To reconcile the ESS  $^{92}\text{Nb}$  abundance with an isolation time of 15 Myr, the half life of  $^{92}\text{Nb}$  should be almost a factor of three higher, which seems unrealistic. The current half life is the weighted average of two experiments that produced similar results in spite of being based on different normalizations: the first [45] is normalized to the half life of  $^{94}\text{Nb}$ , which is not well known, and the second [46] to an assumed value of the  $^{93}\text{Nb}(n, 2n)^{92}\text{Nb}$  cross section. Another option is that the  $^{92}\text{Nb}/^{92}\text{Mo}$  ratio in the ESS is lower than  $2.2 \times 10^{-5}$ , i.e., 21% lower than the current lower limit. It is harder to reconcile the different  $T_{\text{mixing}}$ : when using the lowest ( $K=1$ ) ISM  $^{53}\text{Mn}/^{55}\text{Mn}$  ratio and the upper limit for the ESS ratio, we obtain a lower limit for  $T_{\text{mixing}}$  of 24 Myr. To reconcile the  $^{92}\text{Nb}/^{92}\text{Mo}$  ratio to this timescale an ESS  $^{92}\text{Nb}/^{92}\text{Mo}=1.6 \times 10^{-5}$  is required, 43% lower than the current lower limit. A different solution is to look into another production site for  $^{92}\text{Nb}$ .

### The CCSN source

As mentioned above, the  $\gamma$ -process in CCSN models do not efficiently produce  $p$ -process isotopes in the Mo-Ru region, but, other CCSN nucleosynthesis components may contribute to these isotopes. Pignatari *et al.* 2013 [47] computed CCSN models with initial mass of  $15 M_{\odot}$  that carry in the ejecta an  $\alpha$ -rich freezeout component. There, production of the  $p$ -process nuclei up to  $^{92}\text{Mo}$  occurs due to a combination of  $\alpha$ , proton, and neutron captures and their inverse reactions during the CCSN explosion in the deepest part of the ejecta, where  $^4\text{He}$  is the most abundant isotope. The stellar evolution before the CCSN explosion was calculated with the code GENECS [48] and the explosion simulations were based on the prescriptions for shock velocity and fallback by [49]. The standard initial shock velocity used beyond fallback is  $2 \times 10^9 \text{ cm s}^{-1}$  for all the masses, and we also experimented by reducing it down to 200 times lower. Results are presented for CCSN models computed with two setups for the convection-enhanced neutrino-driven explosion: fast-convection (the rapid setup) and delayed-convection (the delay setup) explosions [49]. In this framework, nuclear uncertainties are insignificant compared to model uncertainties. A post-processing code was used to calculate the nucleosynthesis before and during the explosion [50]. The results are summarized and compared to the SNIa models in Figure 1.

In comparison to the SNIa models, the CCSN models produce less  $^{53,55}\text{Mn}$ ,  $^{56}\text{Fe}$ , and  $^{144,146}\text{Sm}$ , and almost no  $^{98}\text{Ru}$  and  $^{97,98}\text{Tc}$ . On the other hand, no  $^{60}\text{Fe}$  is produced in SNeIa, and the cosmic origin of this isotope has to be ascribed to other types of supernovae, including CCSNe. Significant production of  $^{92}\text{Nb}$  and  $^{92}\text{Mo}$  occurs in CCSN models of  $15 M_{\odot}$ , with production factors for  $^{92}\text{Mo}$  comparable to those of the SNIa models, and  $^{92}\text{Nb}/^{92}\text{Mo}$  ratios up to five times higher. CCSN models with initial mass larger than  $15 M_{\odot}$  do not eject material exposed to the  $\alpha$ -rich freezeout due to the more extended fallback. The  $\alpha$ -rich freezeout efficiency also strongly depends on the shock velocity. When its standard value is reduced, even only by a factor of two, the amounts of  $^{92}\text{Mo}$  and  $^{92}\text{Nb}$  ejected become negligible. This is because for lower shock velocities the bulk of  $\alpha$ -rich freezeout nucleosynthesis is shifted

toward lighter elements closer to the Fe group. Only some  $\gamma$ -process component is produced in these cases, which is poor in  $^{92}\text{Mo}$ . In summary, the  $\alpha$ -rich freezeout conditions suitable to produce  $^{92}\text{Mo}$  and  $^{92}\text{Nb}$  are more likely hosted in CCSNe with initial mass of  $15 M_{\odot}$  or lower and shock velocities at least as large as those provided by [49].

We explored the possibility that the  $^{92}\text{Nb}$  in the ESS came from the  $\alpha$  freezeout production experienced by these  $15 M_{\odot}$  CCSN models. Since the premise of Eq. 1 is that both the stable and unstable isotopes present in the ESS were produced only by this type of event, under such assumption, we can apply Eq. 1 only to calculate the  $^{92}\text{Nb}/^{92}\text{Mo}$  ratios to derive the time of the last such  $\alpha$  freezeout event, since the other isotopes are not produced in any significant abundances<sup>2</sup>. The calculations are hampered by the error bars on the ESS ratios and the large uncertainties related to the choice of the free parameters entering in Eq. 1. However, to infer further information on the birth of the Sun we are particularly interested in determining the lower limit of  $T_{\text{last}}$  because this provides us the shortest possible timescale, within all the uncertainties above, for the life of the star forming region where the Sun was born. Using  $K=1$  in Eq. 1 and the upper limit of the ESS  $^{92}\text{Nb}/^{92}\text{Mo}$  ratio we inferred a lower limit for  $T_{\text{last}}$  of 10 Myr when using the delay setup CCSN model (Table 2). However, we stress that  $K=1$  represents a very conservative lower limit because the production factor  $^{92}\text{Mo}/^{92}\text{Mo}_{\odot}$  of the CCSN delay model is comparable to that of the SNIa model (140 versus 172). This means that we would need a similar number of events (which scales as  $1/K\delta$ ) to reproduce the  $^{92}\text{Mo}$  solar abundance - although the exact value would depend on the metallicity dependence of  $^{92}\text{Mo}/^{92}\text{Mo}_{\odot}$  in the CCSN models, which we did not explore. The lower limit of  $T_{\text{last}}$  from the rapid setup CCSN model is instead a negative value. However, the production factor  $^{92}\text{Mo}/^{92}\text{Mo}_{\odot}$  of the rapid model is five times higher than that of the delay model (704 versus 140). This means that we would need five times less events to reach the same value of  $^{92}\text{Mo}$  in the Solar System, hence, for consistency, a five times higher value of  $1/K\delta$  is more appropriate in this case. If we use, e.g.,  $\delta=50$  Myr we obtain 7 Myr as the conservative lower limit for  $T_{\text{last}}$ .

## Discussion

Our models show that  $^{146}\text{Sm}$  in the ESS was produced by SNIa events, together with  $^{97,98}\text{Tc}$ . The large nuclear uncertainties on the former and the availability of upper limits only for the ESS ratio for the latter two do not allow us to derive precise timescales. On the other hand, to reconcile the abundances of  $^{53}\text{Mn}$  and  $^{92}\text{Nb}$  in the ESS as produced primarily by SNIa events, the ESS  $^{92}\text{Nb}/^{92}\text{Mo}$  ratio needs to be at least 50% lower than the current nominal value, which is outside its present error bars. In this case  $T_{\text{isolation}} \simeq 15$  Myr, which is consistent with the  $T_{\text{last}}$  derived for the last  $r$  ( $\sim 100$  Myr) and  $s$  ( $\sim 20$  Myr) process events [2] since  $T_{\text{last}}$  represents an upper limit for  $T_{\text{isolation}}$ . Furthermore, if all the  $^{53}\text{Mn}$  in the ESS was produced by the same SNIa events that produced  $^{92}\text{Nb}$ , no CCSNe exploding within the star-forming region where the Sun was born should have contributed to the abundances of radioactive nuclei in the ESS, since they would have contributed extra  $^{53}\text{Mn}$ . If correct, this will have important consequences for the origin of  $^{26}\text{Al}$  and  $^{60}\text{Fe}$  in the ESS. The  $^{60}\text{Fe}/^{56}\text{Fe}$  is likely the result of the decay, after a certain isolation time, of the  $^{60}\text{Fe}$  abundance in the ISM. This is consistent with the direct observational constraint from  $\gamma$ -ray astronomy of  $^{60}\text{Fe}/^{56}\text{Fe} \simeq 2.8 \times 10^{-7}$  in the ISM, and with timescales of the order of 15 Myr, while  $^{26}\text{Al}$  may have originated from the winds of a massive star [51].

Another possibility is that the  $^{92}\text{Nb}$  was instead predominantly produced by CCSNe that experienced the  $\alpha$ -rich freezeout, corresponding in our models to low initial stellar masses experiencing a core-collapse with high shock velocities. In the extreme scenario where all the  $^{92}\text{Nb}$  and  $^{92}\text{Mo}$  in the ESS came from such events we have derived lower limits for the timing of the last of them. These are also still consistent with a relatively long  $T_{\text{isolation}}$  of at least 7 Myr, since  $T_{\text{isolation}} \sim T_{\text{last}}$  when  $\delta \ll \tau$ , which is verified for  $^{92}\text{Nb}$  when  $\delta=10$  Myr.

Clearly,  $^{92}\text{Nb}$  could have been produced by both SNIa and CCSN events. Full GCE models are required, including both SNIa, the  $\alpha$ -rich freezeout component of CCSN considered here, and the possible production in the neutrino winds. Because the  $\alpha$ -rich freezeout CCSNe events of initial mass  $15 M_{\odot}$  produce higher amounts of  $^{92}\text{Nb}$  than SNIa, we expect that adding them to the balance will increase the ISM  $^{92}\text{Nb}/^{92}\text{Mo}$  ratio at the time of the formation of the Solar System, leading to longer  $T_{\text{isolation}}$ , and an easier match with the  $^{53}\text{Mn}/^{55}\text{Mn}$  constraint. In conclusion, a higher-precision determination of the ESS  $^{92}\text{Nb}/^{92}\text{Mo}$  ratio is urgently required. This will allow us to determine if SNIa are the major source of light  $p$ -process nuclei in the Galaxy or if CCSNe also play a role; and which fraction of the  $^{53}\text{Mn}$  in the ESS originated from SNIa.

**ACKNOWLEDGMENTS.** ML is a Momentum (“Lendület-2014” Programme) project leader of the Hungarian Academy of Sciences. MP acknowledges support to NuGrid from NSF grants PHY 09-22648 (Joint Institute for Nuclear Astrophysics, JINA), NSF grant PHY-1430152 (JINA Center for the Evolution of the Elements) and EU MIRGCT-2006-046520. MP acknowledges the support from the “Lendület-2014” Programme of the Hungarian Academy of Sciences (Hungary) and from SNF (Switzerland).

## References

1. Dauphas N, Chaussidon M (2011) A Perspective from Extinct Radionuclides on a Young Stellar Object: The Sun and Its Accretion Disk. *Annual Review of Earth and Planetary Sciences* 39:351–386.
2. Lugaro M et al. (2014) Stellar origin of the  $^{182}\text{Hf}$  cosmochronometer and the presolar history of solar system matter. *Science* 345:650–653.
3. Murray N (2011) Star Formation Efficiencies and Lifetimes of Giant Molecular Clouds in the Milky Way. *Astrophys. J.* 729:133.
4. Arnould M, Goriely S (2003) The  $p$ -process of stellar nucleosynthesis: astrophysics and nuclear physics status. *Phys. Rep.* 384:1–84.
5. Rauscher T et al. (2013) Constraining the astrophysical origin of the  $p$ -nuclei through nuclear physics and meteoritic data. *Reports on Progress in Physics* 76:066201.
6. Woosley SE, Heger A, Weaver TA (2002) The evolution and explosion of massive stars. *Reviews of Modern Physics* 74:1015–1071.
7. Woosley SE, Howard WM (1978) The  $p$ -process in supernovae. *Astrophys. J. Suppl.* 36:285–304.
8. Prantzos N, Hashimoto M, Rayet M, Arnould M (1990) The  $p$ -process in SN 1987 A. *Astron. Astrophys.* 238:455–461.
9. Rayet M, Arnould M, Hashimoto M, Prantzos N, Nomoto K (1995) The  $p$ -process in Type II supernovae. *Astron. Astrophys.* 298:517–527.
10. Rauscher T, Heger A, Hoffman RD, Woosley SE (2002) Nucleosynthesis in Massive Stars with Improved Nuclear and Stellar Physics. *Astrophys. J.* 576:323–348.
11. Rapp W, Görres J, Wiescher M, Schatz H, Käppeler F (2006) Sensitivity of  $p$ -Process Nucleosynthesis to Nuclear Reaction Rates in a  $25 M_{\text{Solar}}$  Supernova Model. *Astrophys. J.* 653:474–489.

<sup>2</sup>Even if all the Mn came from these events we would obtain timescales consistent with those derived from  $^{92}\text{Nb}$ .

12. Rauscher T (2006) Branchings in the  $\gamma$  process path revisited. *Phys. Rev. C* 73:015804.
13. Bennett ME et al. (2012) The effect of  $^{12}\text{C} + ^{12}\text{C}$  rate uncertainties on the evolution and nucleosynthesis of massive stars. *Mon. Not. R. Astron. Soc.* 420:3047–3070.
14. Pignatari M et al. (2013) The  $^{12}\text{C} + ^{12}\text{C}$  Reaction and the Impact on Nucleosynthesis in Massive Stars. *Astrophys. J.* 762:31.
15. Woosley SE, Hoffman RD (1992) The alpha-process and the r-process. *Astrophys. J.* 395:202–239.
16. Hoffman RD, Woosley SE, Fuller GM, Meyer BS (1996) Production of the Light p-Process Nuclei in Neutrino-driven Winds. *Astrophys. J.* 460:478–488.
17. Farouqi K, Kratz KL, Pfeiffer B (2009) Co-Production of Light p-, s- and r-Process Isotopes in the High-Entropy Wind of Type II Supernovae. *Publ. Astron. Soc. Austr.* 26:194–202.
18. Arcones A, Montes F (2011) Production of Light-element Primary Process Nuclei in Neutrino-driven Winds. *Astrophys. J.* 731:5.
19. Fröhlich C et al. (2006) Nucleosynthesis in neutrino-driven supernovae. *New Astron. Rev.* 50:496–499.
20. Fisker JL, Hoffman RD, Pruet J (2009) On the Origin of the Lightest Molybdenum Isotopes. *Astrophys. J. Lett.* 690:L135–L139.
21. Dauphas N, Rauscher T, Marty B, Reisberg L (2003) Short-lived p-nuclides in the early solar system and implications on the nucleosynthetic role of X-ray binaries. *Nuclear Physics A* 719:287c.
22. Hayakawa T et al. (2013) Supernova neutrino nucleosynthesis of the radioactive  $^{92}\text{Nb}$  observed in primitive meteorites. *Astrophys. J. Lett.* 779:L9.
23. Kusakabe M, Iwamoto N, Nomoto K (2011) Production of the p-process Nuclei in the Carbon-deflagration Model for Type Ia Supernovae. *Astrophys. J.* 726:25.
24. Travaglio C, Röpke FK, Gallino R, Hillebrandt W (2011) Type Ia Supernovae as Sites of the p-process: Two-dimensional Models Coupled to Nucleosynthesis. *Astrophys. J.* 739:93.
25. Travaglio C, Gallino R, Rauscher T, Röpke FK, Hillebrandt W (2015) Testing the Role of SNe Ia for Galactic Chemical Evolution of p-nuclei with Two-dimensional Models and with s-process Seeds at Different Metallicities. *Astrophys. J.* 799:54.
26. Travaglio C et al. (2014) Radiogenic p-isotopes from Type Ia Supernova, Nuclear Physics Uncertainties, and Galactic Chemical Evolution Compared with Values in Primitive Meteorites. *Astrophys. J.* 795:141.
27. Wasserburg GJ, Busso M, Gallino R, Nollett KM (2006) Short-lived nuclei in the early Solar System: Possible AGB sources. *Nuclear Physics A* 777:5–69.
28. Meyer BS, Clayton DD (2000) Short-Lived Radioactivities and the Birth of the sun. *Space Sci. Rev.* 92:133–152.
29. Clayton DD (1985) *Galactic Chemical Evolution and Nucleocosmochronology: A Standard Model* eds. Arnett WD, Truran JW. p. 65.
30. Huss GR, Meyer BS, Srinivasan G, Goswami JN, Sahijpal S (2009) Stellar sources of the short-lived radionuclides in the early solar system. *Geochim. Cosmochim. Acta* 73:4922–4945.
31. Clayton DD (1983) Extinct radioactivities - A three-phase mixing model. *Astrophys. J.* 268:381–384.
32. Casagrande L et al. (2011) New constraints on the chemical evolution of the solar neighbourhood and Galactic disc(s). Improved astrophysical parameters for the Geneva-Copenhagen Survey. *Astron. Astrophys.* 530:A138.
33. Sánchez-Blázquez P, Courty S, Gibson BK, Brook CB (2009) The origin of the light distribution in spiral galaxies. *Mon. Not. R. Astron. Soc.* 398:591–606.
34. Kobayashi C, Nakasato N (2011) Chemodynamical Simulations of the Milky Way Galaxy. *Astrophys. J.* 729:16.
35. Somorjai E et al. (1998) Experimental cross section of  $^{144}\text{Sm}(\alpha, \gamma)^{148}\text{Gd}$  and implications for the p-process. *Astron. Astrophys.* 333:1112–1116.
36. Rauscher T, Thielemann FK (2000) Astrophysical Reaction Rates From Statistical Model Calculations. *Atomic Data and Nuclear Data Tables* 75:1–351.
37. Rauscher T (2013) Solution of the  $\alpha$ -Potential Mystery in the  $\gamma$  Process and Its Impact on the Nd/Sm Ratio in Meteorites. *Physical Review Letters* 111(6):061104.
38. Gyürky G, Fülöp Z, Halász Z, Kiss GG, Szücs T (2014) Direct study of the  $\alpha$ -nucleus optical potential at astrophysical energies using the  $^{64}\text{Zn}(p, \alpha)^{61}\text{Cu}$  reaction. *Phys. Rev. C* 90:052801.
39. Kinoshita N et al. (2012) A Shorter  $^{146}\text{Sm}$  Half-Life Measured and Implications for  $^{146}\text{Sm}$ - $^{142}\text{Nd}$  Chronology in the Solar System. *Science* 335:1614–1617.
40. Marks NE, Borg LE, Hutcheon ID, Jacobsen B, Clayton RN (2014) Samarium-neodymium chronology and rubidium-strontium systematics of an Allende calcium-aluminum-rich inclusion with implications for  $^{146}\text{Sm}$  half-life. *Earth and Planetary Science Letters* 405:15–24.
41. Seitenzahl IR, Cescutti G, Röpke FK, Ruiter AJ, Pakmor R (2013) Solar abundance of manganese: a case for near Chandrasekhar-mass Type Ia supernova progenitors. *Astron. Astrophys.* 559:L5.
42. Travaglio C, Hillebrandt W, Reinecke M, Thielemann FK (2004) Nucleosynthesis in multi-dimensional SN Ia explosions. *Astron. Astrophys.* 425:1029–1040.
43. Parikh A, José J, Seitenzahl IR, Röpke FK (2013) The effects of variations in nuclear interactions on nucleosynthesis in thermonuclear supernovae. *Astron. Astrophys.* 557:A3.
44. Dressler R et al. (2012)  $^{44}\text{Ti}$ ,  $^{26}\text{Al}$  and  $^{53}\text{Mn}$  samples for nuclear astrophysics: the needs, the possibilities and the sources. *Journal of Physics G Nuclear Physics* 39:105201.
45. Makino T, Honda M (1977) Half-life of  $^{92}\text{Nb}$ . *Geochim. Cosmochim. Acta* 41:1521–1523.
46. Nethaway DR, Prindle AL, van Konynenburg RA (1978) Half-life of  $^{92}\text{Nb}^{\beta}$ . *Phys. Rev. C* 17:1409–1413.
47. Pignatari M et al. (2013) NuGrid stellar data set. I. Stellar yields from H to Bi for stars with metallicities  $Z = 0.02$  and  $Z = 0.01$ . *ArXiv e-prints: 1307.6961*.
48. Eggenberger P et al. (2008) The Geneva stellar evolution code. *Astrophys. Space Sci.* 316:43–54.
49. Fryer CL et al. (2012) Compact Remnant Mass Function: Dependence on the Explosion Mechanism and Metallicity. *Astrophys. J.* 749:91.
50. Pignatari M, Herwig F (2012) The NuGrid Research Platform: A Comprehensive Simulation Approach for Nuclear Astrophysics. *Nuclear Physics News* 22(4):18–23.
51. Tang H, Dauphas N (2012) Abundance, distribution, and origin of  $^{60}\text{Fe}$  in the solar protoplanetary disk. *Earth and Planetary Science Letters* 359-360:248–263.
52. Trinquier A, Bircck JL, Allègre CJ, Göpel C, Ulfbeck D (2008)  $^{53}\text{Mn}$ - $^{53}\text{Cr}$  systematics of the early Solar System revisited. *Geochim. Cosmochim. Acta* 72:5146–5163.
53. Tang H, Dauphas N (2015) Low  $^{60}\text{Fe}$  Abundance in Semarkona and Sahara 99555. *Astrophys. J.* 802:22.
54. Harper, Jr. CL (1996) Evidence for  $^{92}\text{gNb}$  in the Early Solar System and Evaluation of a New p-Process Cosmochronometer from  $^{92}\text{gNb}/^{92}\text{Mo}$ . *Astrophys. J.* 466:437–456.
55. Lodders K, Palme H, Gail HP (2009) Abundances of the Elements in the Solar System. *Landolt-Börnstein, New Series VI/4B, 34, Chapter 4.4*.
56. Dauphas N, Marty B, Reisberg L (2002) Molybdenum Evidence for Inherited Planetary Scale Isotope Heterogeneity of the Protosolar Nebula. *Astrophys. J.* 565:640–644.
57. Becker H, Walker RJ (2003) In search of extant Tc in the early solar system:  $^{98}\text{Ru}$  and  $^{99}\text{Ru}$  abundances in iron meteorites and chondrites. *Chemical Geology* 196:43–56.
58. Boyet M, Carlson RW, Horan M (2010) Old Sm-Nd ages for cumulate eucrites and redetermination of the solar system initial  $^{146}\text{Sm}/^{144}\text{Sm}$  ratio. *Earth and Planetary Science Letters* 291:172–181.
59. Göpel C, Bircck JL, Galy A, Barrat JA, Zanda B (2015) Mn-Cr systematics in primitive meteorites: Insights from mineral separation and partial dissolution. *Geochim. Cosmochim. Acta* 156:1–24.

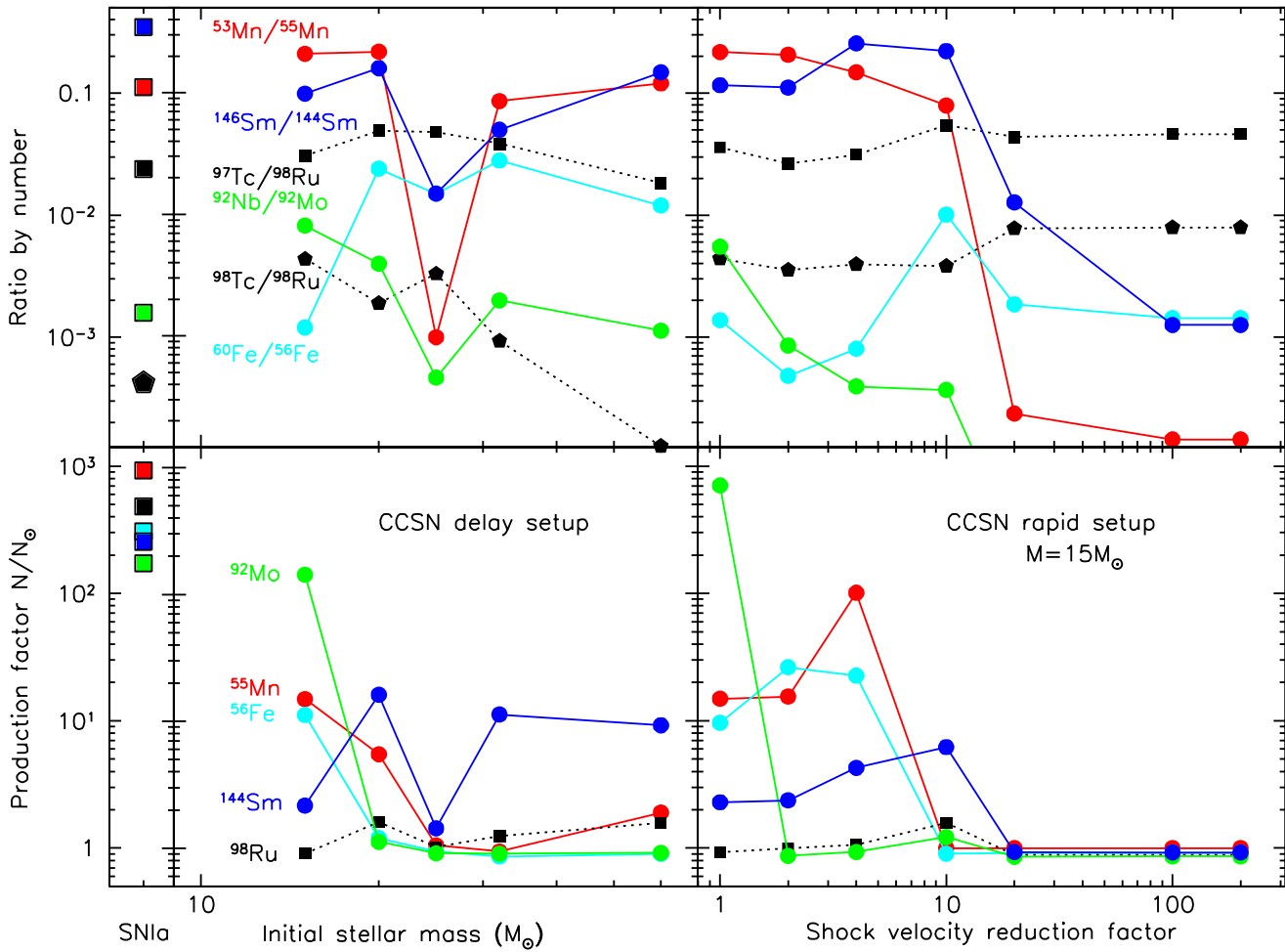


**Fig. 1.** Results for the radioactive and stable nuclei of interest from the CCSN models as compared to those from SNIa (TR14). The CCSN models with the delay setup have initial masses 15, 20, 25, 32 and 60  $M_{\odot}$  and metallicity 0.02. The CCSN models with the rapid setup are for a star of initial mass 15  $M_{\odot}$  and different reduction factors for the shock velocity. The rate by [36] was used for the  $^{148}\text{Gd}(\gamma, \alpha)^{144}\text{Sm}$  reaction. As mentioned in the text, using the new rate by [37] would result in  $^{146}\text{Sm}/^{144}\text{Sm}$  ratios higher in SNIa and lower in CCSNe.

**Table 1.** Decay rates, ESS ratios, SNIa production and ISM ratios, and timescales for the isotopes of interest

	$^{53}\text{Mn}$	$^{60}\text{Fe}$	$^{92}\text{Nb}$	$^{97}\text{Tc}$	$^{98}\text{Tc}$	$^{146}\text{Sm}$
$T_{1/2}$ (Myr)	3.7	2.6	35	4.2	4.2	68
$\tau$ (Myr)	5.3	3.8	50	6.1	6.1	98
reference isotope	$^{55}\text{Mn}$	$^{56}\text{Fe}$	$^{92}\text{Mo}$	$^{98}\text{Ru}$	$^{98}\text{Ru}$	$^{144}\text{Sm}$
ESS ratio	$(6.28 \pm 0.66) \times 10^{-6}$	$(5.39 \pm 3.27) \times 10^{-9}$	$(3.4 \pm 0.6) \times 10^{-5}$	$< 4 \times 10^{-5}$	$< 6 \times 10^{-5}$	$(9.4 \pm 0.5) \times 10^{-3}$
reference	[52]*	[53]	[54, 55]	[55, 56]	[55, 57]	[26, 58]
production ratio <sup>†</sup>	0.108	$< 10^{-9}$	$1.58 \times 10^{-3}$	$2.39 \times 10^{-2}$	$4.22 \times 10^{-4}$	0.347
ISM from GCE <sup>‡</sup>			$1.72^{+1.40}_{-0.06} \times 10^{-5}$	$4.08 \times 10^{-5}$	$6.47 \times 10^{-7}$	$7.0^{+9.7} \times 10^{-3}$
ISM from Eq. 1 <sup>§</sup>	$2.41 \times 10^{-4}$	$< 10^{-12}$	$1.86 \times 10^{-5}$	$5.68 \times 10^{-5}$	$1.00 \times 10^{-6}$	$7.70 \times 10^{-3}$
$T_{\text{isolation}}$ <sup>¶</sup>	19 – 20	-	$\leq 5.4$	$> 0.12$	-	$\leq 62$
$T_{\text{mixing}}$	40 – 45	-	$\leq 3.7$	$> 0.08$	-	$\leq 50$

\* The most recent value of  $6.8 \times 10^{-6}$  given by [59] is included in the given error bars.

<sup>†</sup> Average of the ratios from Table 1 of TR14 from metallicities from 0.01 to 0.02, except for  $^{53}\text{Mn}/^{55}\text{Mn}$  from [24] and  $^{60}\text{Fe}/^{56}\text{Fe}$  from [42].

<sup>‡</sup> From Tables 2, 3, and 4 of TR14

<sup>§</sup> Using  $K=2$ ,  $\delta = 8$  Myr, and  $T=9200$  Myr.

<sup>¶</sup> Reported ranges reflect the error bars on the ESS and ISM ratios.

**Table 2.**  $^{92}\text{Nb}/^{92}\text{Mo}$  from the CCSN models of  $15 M_{\odot}$ , ISM ratios, and inferred lower limits for  $T_{\text{last}}$

production ratios	delay setup			rapid setup		
	$\delta = 10 \text{ Myr}$	$\delta = 50 \text{ Myr}$	$\delta = 100 \text{ Myr}$	$\delta = 10 \text{ Myr}$	$\delta = 50 \text{ Myr}$	$\delta = 100 \text{ Myr}$
ISM ratio*	$4.92 \times 10^{-5}$	$7.06 \times 10^{-5}$	$1.03 \times 10^{-4}$	$3.18 \times 10^{-5}$	$4.56 \times 10^{-5}$	$6.66 \times 10^{-5}$
lower limit of $T_{\text{last}}^{\dagger}$	10	29	48	-	7	25

\*From Eq. 1 using  $T=9200 \text{ Myr}$  and  $K=1$  to obtain a conservative lower limit.

$\dagger$ Using the ESS upper limit of  $4.0 \times 10^{-5}$ .